Journal of Computer-Aided Molecular Design (2005) 19: 123–136
DOI 10.1007/s10822-005-2998-9

5,10-Methylene-5,6,7,8-tetrahydrofolate conformational transitions upon binding to thymidylate synthase: molecular mechanics and continuum solvent studies

Adam Jarmuła[1,2,*], Piotr Cieplak[3,4] & William R. Montfort[2]
[1]*Nencki Institute of Experimental Biology, Polish Academy of Sciences, 3 Pasteur St., 02-093 Warszawa, Poland;* [2]*Department of Biochemistry and Molecular Biophysics, University of Arizona, Tucson, Arizona 85721, USA;* [3]*The Burnham Institute, 10901 N. Torrey Pines Road, La Jolla, California 92037, USA;* [4]*Department of Chemistry, Warsaw University, 1 Pasteur St., 02-093 Warszawa, Poland*

Received 20 May 2004; accepted 24 February 2005

Key words: 5,10-methylene-5,6,7,8-tetrahydrofolate, conformational transitions, free energies in aqueous solution, molecular mechanics Poisson–Boltzmann surface area (MM-PBSA) approach, thymidylate synthase

Summary

We applied the molecular mechanics Poisson–Boltzmann surface area (MM-PBSA) approach to evaluate relative stability of the extended (flat) and C-shaped (bent) *solution* conformational forms of the 5,10-methylene-5,6,7,8-tetrahydrofolate (mTHF) molecule in aqueous solution. Calculations indicated that both forms have similar free energies in aqueous solution but detailed energy components are different. The bent *solution* form has lower intramolecular electrostatic and van der Waals interaction energies. The flat form has more favorable solvation free energy and lower contribution from the bond, angle and torsion angle molecular mechanical internal energies. We exploit these results and combine them with known crystallographic data to provide a model for the progressive binding of the mTHF molecule, a natural cofactor of thymidylate synthase (TS), to the complex forming in the TS-catalyzed reaction. We propose that at the time of initial weak binding in the open enzyme the cofactor molecule remains in a close balance between the flat and bent *solution* conformations, with neither form clearly favored. Later, thymidylate synthase undergoes conformational change leading to the closure of the active site and the mTHF molecule is withdrawn from the solvent. That effect shifts the thermodynamic equilibrium of the mTHF molecule toward the bent *solution* form. At the same time, burying the cofactor molecule in the closed active site produces numerous contacts between mTHF and protein that render change in the shape of the mTHF molecule. As a result, the bent *solution* conformer is converted to more strained L-shaped bent *enzyme* conformer of the mTHF molecule. The strain in the bent *enzyme* conformation allows for the tight binding of the cofactor molecule to the productive ternary complex that forms in the closed active site, and facilitates the protonation of the imidazolidine N10 atom, which promotes further reaction.

Abbreviations: CH_2H_4Folate or mTHF – 5,10-methylene-5,6,7,8-tetrahydrofolate; dUMP – 2′-deoxyuridine 5′-monophosphate; FdUMP – 5-fluoro-dUMP; GB – generalized Born; MD – molecular dynamics; MM-PBSA – molecular mechanics Poisson–Boltzmann surface area; NO_2dUMP – 5-nitro-dUMP; PB – Poisson–Boltzmann; RESP – restrained electrostatic potential; SASA – solvent-accessible surface area; TS – thymidylate synthase.

*To whom correspondence should be addressed. Fax: +4822-822-5342; E-mail: a.jarmula@nencki.gov.pl

Introduction

Thymidylate synthase (TS) (EC 2.1.1.45) is an enzyme of long standing and continuous appeal for its central role in DNA synthesis as well as for many interesting mechanistic features, some of them well known, others remaining yet to be explored (reviewed in papers by Pogolotti and Santi [1], Santi and Danenberg [2], Carreras and Santi [3], Hardy [4], Hyatt et al. [5], Montfort and Weichsel [6], Stroud and Finer-Moore [7], and Finer-Moore et al. [8]). Thymidylate synthase catalyzes the conversion of 2′-deoxyuridine-5′-monophosphate (dUMP) and 5,10-methylene-5,6,7,8-tetrahydrofolate (CH_2H_4Folate, or mTHF) to 2′-deoxythymidine-5′-monophosphate (dTMP) and 7,8-dihydrofolate (H_2Folate, or DHF) by reductive methylation, in which mTHF serves as both methyl donor and reducing agent. Until the recent discovery of a protein called thymidylate synthase complementing protein (TSCP) [9], this reaction has been thought to be the sole *de novo* biosynthetic source of thymine in DNA. The inhibition of TS in rapidly dividing cells, in the absence of preformed thymidine, blocks DNA synthesis, and eventually leads to cell death, a phenomenon termed 'thymineless death' [10]. As a consequence, TS has been a logical and uniquely suited target for the design of chemotherapeutic agents [11]. In search for specific and non-toxic inhibitors of TS, compounds modeled after both dUMP [12–16] and mTHF [17–20], as well as novel classes of inhibitors [21–25], have been studied, with 5-fluorouracil [26, 27] (after metabolic conversion to 5-fluoro-dUMP (FdUMP)) and folate-based raltitrexed (Tomudex, ZD1694) [18] approved for therapies, and many others, especially antifolates, in different stages of clinical trials. Studies leading scientists to the design of these inhibitors, initiated from simple chemical model systems, kinetic measurements, and spectroscopic data, and more recently reinforced by availability of three-dimensional structures from crystallographic experiments and structure-based design, have resulted in a proposed mechanism of reaction for thymidylate synthase, shown in Figure 1.

During catalysis, TS undergoes a substantial conformational change that leads to complete burial of both dUMP and mTHF. Such conformational changes are commonplace, yet the roles they play in catalysis are poorly understood. Here, we applied molecular mechanics Poisson–Boltzmann surface area (MM-PBSA) approach [28–31] to investigate the energetics of mTHF bending in the active site of TS in order to explore the consequences of conformational change in a well-studied system. As illustrated in Figure 1, the TS reaction has an ordered mechanism, with dUMP being bound before mTHF, and dTMP released from the product complex after DHF. Initially bound and properly oriented dUMP forms a binding surface against which the pterin ring of mTHF binds [32, 33]. Crystallographic structures of TS ternary complexes in the productive conformation, show the cofactor in strongly bent (L-shaped) conformation, with the PABA ring 'folded back' toward the pterin ring, and the imidazolidine ring broken. This conformation differs from the unbound conformation of mTHF, which according to the NMR [34] and crystallographic [35] reports is relatively flat, with the PABA ring extended away from the pterin ring, rather than being 'folded back'. The imminium ion of mTHF formed after initial protonation and subsequent opening of the imidazolidine ring has been postulated to form during the ligand-induced conformational change of TS and before the active site closure [36, 37]. It has been argued that the imidazolidine ring would be too strained to exist in the highly bent, productive conformation with an intact imidazolidine ring. Yet, opposite arguments have been raised as well. In a pre-steady-state kinetics study, Spencer et al. [38] found that the equilibrium among the bound cofactor intermediates would favor unaltered mTHF i.e., the mTHF molecule with the imidazolidine ring closed. Furthermore, it has been shown that the imminium cation that is formed from mTHF is reactive, and its estimated short lifetime in aqueous solution suggests that the methylene group transfer from mTHF in the TS reaction may proceed through a concerted mechanism in which formation of the free imminium ion is circumvented [39]. Recently, the crystallographic structure of the ternary complex of TS with the substrate analogue 5-nitro-dUMP (NO_2dUMP), and mTHF, has been investigated. Although somewhat disordered, the data suggest mTHF is bound with the imidazolidine ring intact, as illustrated in Figure 2 [40]. The structure in Figure 2 raises two important questions: By what means does the cofactor adopt such

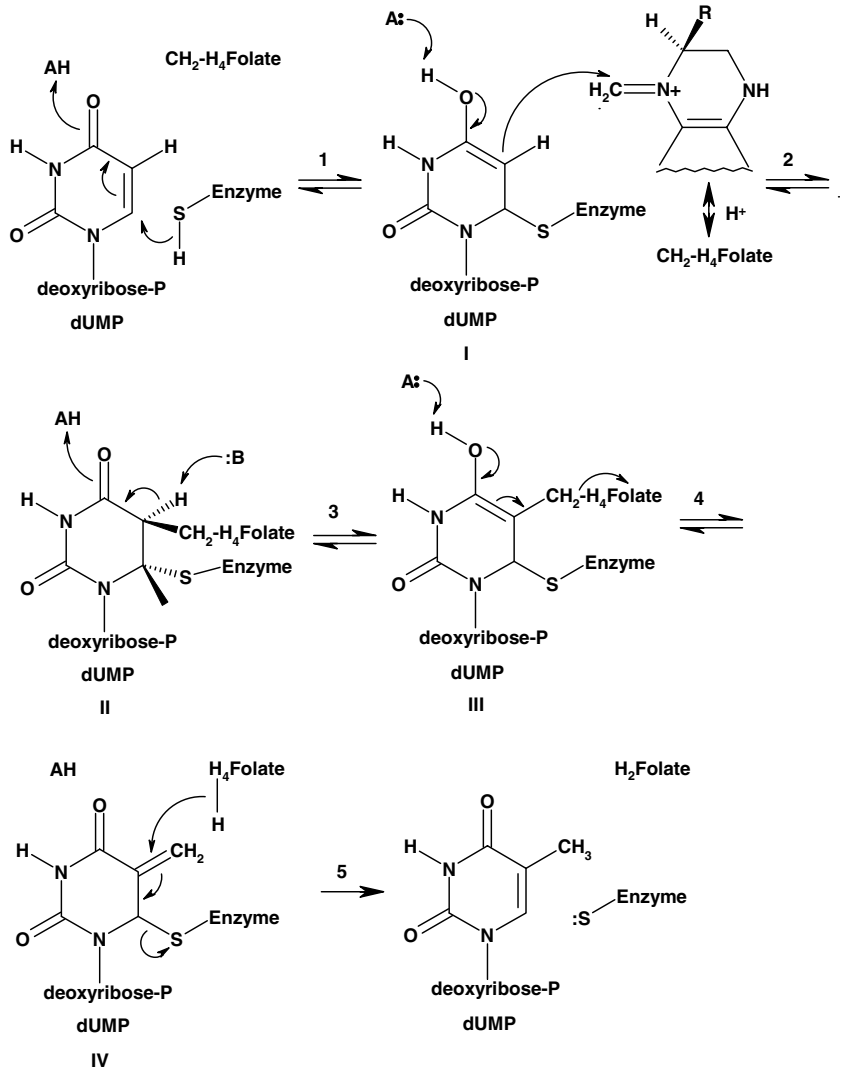

Figure 1. Catalytic mechanism of thymidylate synthase. [8] Substrates, intermediates I–IV, and products of the reaction are shown. 1 to 5 denote the reaction steps 1–5. AH and A: are general acid protonated and deprotonated forms, respectively, and :B is a general base. General acid assists in proton transfer that aids methylene transfer to the dUMP base (steps 1–4). General acid is also postulated to serve for donating a proton to CH_2H_4Folate, resulting in conversion of the latter into a reactive imminium cation (pre-step 2). General base on the enzyme is postulated to serve for abstracting a proton from the covalent TS–dUMP–CH_2H_4-Folate intermediate (step 3).

a strained conformation in the TS active site? How does this conformation compare to the known solution conformations of mTHF? The latter question has been addressed in the NMR study of Poe et al. [34]; however that study was not firmly conclusive for the mTHF conformation at neutral pH. In what follows, we address the both questions. We explore the means by which the strained conformation can be stabilized by the protein and present a model for cofactor conformational transitions that accompany binding.

Methods

Molecular dynamics simulations of mTHF

The initial structures of the flat and bent *solution* mTHF conformers were built using the program Insight II [41] and optimized using the AMBER 6.0 molecular modeling software package [42]. Both structures were solvated in a cubic box of water molecules extended up to 10 Å away from the solute. The resulting systems were first

Figure 2. The bent *enzyme* form of the mTHF molecule, found in the crystallographic structure of the TS–NO_2dUMP–mTHF complex. Hydrogen atoms are omitted. The imidazolidine ring is closed and in half-chair conformation. The PABA ring is strongly "folded back" toward the pterin ring, which causes the N10 atom to stick out to the outside and have its lone pair of electrons exposed.

minimized for 500 steps using the conjugate gradient method to remove steric conflicts. The models were then gradually heated to 300 K in three 5 ps intervals (100 K, 200 K and 300 K). Next, the molecular dynamics equilibrations at 300 K for 200 ps, and then the data collection runs for 1000 ps, were carried out.

All simulations were performed using the *SANDER* module of the AMBER 6.0 software package [42]. The Cornell et al. all-atom force field parameters [43] and the TIP3P [44] water model were used. The simulations were performed in the NpT ensemble with a constant temperature of 300 K and constant pressure of 1 atm. The temperature and pressure coupling parameters were both 1 ps. Periodic boundary conditions and an atom-based cutoff of 8 Å for non-bonded van der Waals interactions were applied. The long-range electrostatic interactions were calculated using the particle-mesh Ewald (PME) procedure [45, 46]. A 1 fs time step was used. A total of 1000 snapshots were saved during each data collection run, one snapshot per each 1 ps of molecular dynamics simulation.

AMBER force field parameters for the mTHF molecules were derived using available spectroscopic data and by performing additional *ab initio* HF/6-31g* geometry optimizations using the Gaussian98 program [47]. The force field atom type assignments for both conformers and the complete list of additional force field parameters used in the simulations are available from the authors upon request.

The partial atomic charges for both mTHF conformers were derived from the electrostatic potentials, calculated at the RHF/6-31G* theory level, using the restrained electrostatic potential (RESP) fitting method [48, 49]. The calculated RESP charges for the heavy (non-hydrogen) atoms are reported in Table 1.

Free energy estimations using the MM-PBSA approach

To estimate free energy of the flat and bent *solution* conformers of the mTHF molecule we applied the MM-PBSA molecular dynamics

Table 1. Charges used in the MM-PBSA calculations for the non-hydrogen atoms in the flat and bent *solution* mTHF molecule forms.

Atom	Flat mTHF	Bent mTHF
N1	−0.6424	−0.6585
C2	0.7335	0.6772
N2	−0.9730	−0.9577
N3	−0.4049	−0.3273
C4	0.4528	0.4133
O4	−0.5708	−0.5778
C4A	−0.0184	−0.0418
N5	−0.1631	−0.2795
C6	0.0131	0.0611
C7	−0.0827	−0.0219
N8	−0.4074	−0.4876
C8A	0.2187	0.3138
C9	−0.0388	0.0513
N10	−0.0806	−0.5281
C11	−0.0669	0.2748
C1′	0.0925	−0.0095
C2′	−0.1733	−0.1549
C3′	−0.1733	−0.1549
C4′	−0.0149	0.1462
C5′	−0.1733	−0.1549
C6′	−0.1733	−0.1549
C	0.4941	0.5904
O	−0.6245	−0.6351
N	−0.3686	−0.3994
C_α	−0.0307	−0.0219
CT	0.7389	0.7548
OT1	−0.7818	−0.7902
OT2	−0.7818	−0.7902
C_β	0.0517	0.0736
C_γ	−0.0325	−0.0450
CD	0.7339	0.7471
OD1	−0.8263	−0.8293
OD2	−0.8263	−0.8293

trajectory postprocessing approach. This approach was initially proposed and applied to various molecular systems by Srinivasan et al. [28], Vorobjev et al. [29], and Jayaram et al. [30], and reviewed by Kollman et al. [31]. According to this method, we first carried out molecular dynamics simulations using explicit water solvent molecules and counter ions, applying the protocol described above. After removing water molecules and counter ions from the trajectories the solute snapshots only were analyzed using continuum solvent approach in order to determine appropriate average free energy components over the whole trajectories.

The free energy G for each snapshot is calculated according to the following formulas:

$$G = E_{\text{gas}} + G_{\text{solvation}} - TS \quad (1)$$

$$G_{\text{solvation}} = G_{\text{polar}} + G_{\text{non-polar}} \quad (2)$$

$$E_{\text{gas}} = E_{\text{internal}} + E_{\text{electrostatic}} + E_{\text{vdW}} \quad (3)$$

$$E_{\text{internal}} = E_{\text{bond}} + E_{\text{angle}} + E_{\text{torsion}}, \quad (4)$$

where T is the temperature, S is the entropy of the solute, and E_{bond}, E_{angle} and E_{torsion} are bond length, angle and torsion angle molecular mechanical contributions to the internal energy (E_{internal}) of the solute. The $E_{\text{electrostatic}}$ and E_{vdW} terms are the electrostatic and van der Waals interaction energies, respectively. E_{gas} is the molecular mechanical energy in the gas phase of the solute, and G_{polar} and G_{nonpolar} are the polar and nonpolar contributions to the solvation free energy ($G_{\text{solvation}}$), respectively.

To calculate the energy terms listed above and the average free energy for the flat and bent *solution* conformers of the mTHF molecule in aqueous solution, we analyzed all 1000 snapshots collected during each molecular dynamics simulation. The energies in the gas phase (E_{gas}) were calculated using the *ANAL* module from the AMBER software package. In this case, the infinite cutoffs for all interactions and the Cornell et al. force field parameters [43] were applied. The vibrational contribution to the entropy was estimated using normal mode analysis with the *NMODE* module of AMBER for the minimized solute structures in the absence of solvent and counter ions. The −TS values for the entropy term were calculated only for few snapshots, assuming that the value will not change much over the whole trajectory for this type of molecule. Here, we report separately the values for −TS; reported values for G_{subtotal} are the sum of the remaining terms: $E_{\text{gas}} + G_{\text{solvation}}$. The polar contribution to the solvation free energy was evaluated as the G(PB) term using the finite-difference Poisson–Boltzmann method [50, 51] and the program Delphi II [52], as well as the G(GB) term using the pair wise generalized Born model [53] and the program GB, distributed together with the AMBER modeling package. In the Delphi II calculations an 80% fill of the lattice together with a grid spacing of 0.5 Å and an automatically determined grid size based on the size of the mTHF molecule were applied. A total of 1000 linear iterations were used for each mTHF conformer. A dielectric constant equal to 1 was assigned to the solute (mTHF), which is consistent with the use of the nonpolarizable molecular mechanics force field in our simulations. The solvent dielectric constant was set to 80. The van der Waals radii of the solute atoms were taken from the Cornell et al. force field [43]. The effective van der Waals radii for GB calculations resulted from conversion of the AMBER radii via conversion factor of $1/(2)^{1/6}$, and then multiplication of the resultant radii by the appropriate scale parameters [54]. The nonpolar contribution to the solvation free energy was estimated based on solvent accessible surface area (SASA) using the following equation: $G_{\text{nonpolar}} = \gamma\text{SASA} + b$ [55], where $\gamma_{\text{PB}} = 0.00542$ kcal/Å^2, $\gamma_{\text{GB}} = 0.0072$ kcal/Å^2, $b_{\text{PB}} = 0.92$ kcal/mol, $b_{\text{GB}} = 0$ kcal/mol. The SASA term for the solute snapshots was evaluated using the MSMS program [56].

Results and discussion

Basic results

In this study, we have investigated the free energies of the flat and bent *solution* conformers of the mTHF molecule, which contains two negatively charged carboxylic groups. The minimized forms in the box of water molecules, the *solution* structures, are shown in Figures 3 and 4. The labeling scheme for this molecule is presented in Figure 5. The main results are summarized in Table 2. As noted above, we collected and analyzed data from the 1 ns molecular dynamics (MD) trajectories.

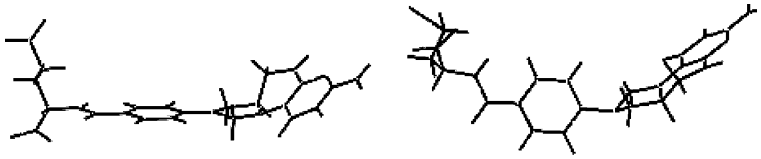

Figure 3. The flat (left) and bent *solution* (right) mTHF forms used in MM-PBSA calculations. Both structures were minimized with the AMBER program. If the conformation of the mTHF molecule in aqueous solution is to be extended (flat) or "folded back" (bent), depends on the hybridization of the imidazolidine N10 atom, which is directly bonded to the aromatic PABA ring. In the flat form, the planar organization of the sp^2 orbital of N10 results in the imidazolidine ring being nearly coplanar with the PABA ring and PABA being extended away from the pterin ring. In the bent conformer, the N10 atom has its sp^3-hybridized orbital in tetrahedral arrangement, which forces PABA to twist out of the plane of the imidazolidine ring, and to slightly "fold back" toward the pterin ring.

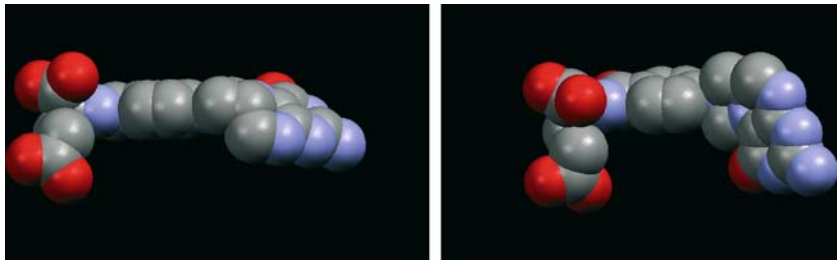

Figure 4. Spacefill representation of the flat, extended (left) and bent *solution*, C-shaped (right) conformations of the mTHF molecule. Carbon atoms are shown in gray, oxygen atoms in red, and nitrogen atoms in blue. Hydrogen atoms are absent.

The average root-mean-square deviations (RMSD) along the trajectories are small and similar for both conformational forms and amount to 1.15 Å and 1.30 Å for flat and bent *solution* mTHF, respectively. In our simulations, we did not observe the conformational transition of one form into the other. The estimated standard deviations for each energy component in Table 2 are similar for both the bent *solution* and flat conformers of the mTHF molecule. On the other hand, the standard deviations are different for particular free energy components, for example lower for electrostatic energies such as $E_{\text{electrostatic}}$ and $G_{\text{solvation}}$ but higher for other components such as E_{internal} and E_{gas}. Apart from any inherent error contributions related to sampling and force field errors, the error range in calculations using the MM-PBSA method depends on the averaging procedure used in a given study [31]. To achieve as much confidence as possible in estimating the apparently very small free energy differences between the flat and bent *solution* conformational forms of the mTHF molecule, we processed every collected snapshot. In this way, we were able to average calculated energies over a large number of 1000 structures. This procedure was likely to mean

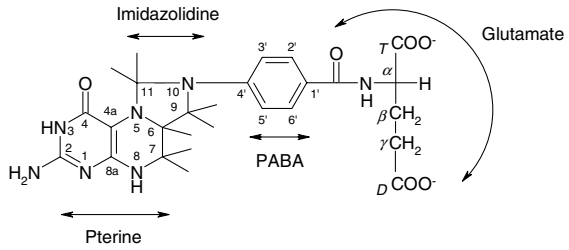

Figure 5. Numbering scheme for the mTHF molecule.

larger standard deviations on the one hand, but more reliable estimates of the free energies on the other hand. Yet, considering the statistical errors and approximate character of the implicit solvation model used in this work, it is quite clear that achieving chemical accuracy could not be the purpose of this study. Our study, however, was aimed to assess the relative free energies. Therefore, both an error cancellation, which is likely to occur when calculating the free energy difference between the conformations, and relative simplicity of the systems and interactions studied here (e.g. no protein involved), would make our results more reliable.

In subsequent sections of this paper we will not take into account the entropy $-TS$ contribution,

Table 2. Free energy terms for the flat and bent *solution* mTHF conformations in aqueous solution.

Contribution	Flat mTHF		Bent mTHF		Notes
	Mean[a]	SD[b]	Mean[a]	SD[b]	
$E_{electrostatic}$	−104.71	4.03	−110.61	4.20	Coulomb energy
E_{vdW}	12.10	1.79	11.51	1.81	Van der Waals energy
$E_{internal}$	51.95	5.53	55.53	5.40	Internal energy
E_{gas}	−40.66	5.82	−43.56	6.06	Total vacuum energy
$G(PB)_{nonpolar}$	4.76	0.04	4.77	0.03	Non-polar solvation
$G(PB)$	−229.36	3.23	−226.65	3.48	Polar solvation
$G(PB)_{solvation}$	−224.60	3.23	−221.89	3.48	Total solvation free energy
$G(PB)_{subtotal}$	−265.26	4.97	−265.45	4.77	$E_{gas} + G(PB)_{solvation}$
$G(GB)_{nonpolar}$	5.10	0.05	5.11	0.04	Non-polar solvation
$G(GB)$	−229.51	3.61	−226.47	3.78	Polar solvation
$G(GB)_{solvation}$	−224.42	3.61	−221.36	3.78	Total solvation free energy
$G(GB)_{subtotal}$	−265.07	5.12	−264.92	4.89	$E_{gas} + G(GB)_{solvation}$
$-TS$[c]	−60.28	NA	−60.40	NA	Entropy term

[a]Average energies from 1000 structures, in kcal/mol.
[b]Standard deviations of the mean energies.
[c]$T = 300$ K.

and will discuss the subtotal $G(PB)_{subtotal}$ and $G(GB)_{subtotal}$ free energy terms as if they were the total free energies. Our normal mode calculations should be considered only as a rough estimate of the entropy (since it is only vibrational contribution estimate) of the solute. Since both conformers are quite similar in terms of normal modes, and the only difference is in less hindered rotation of the PABA ring in the bent *solution* form, the values of the –TS are very similar for both cases (Table 2). The change of conformation from flat to bent *solution* is related to rather moderate changes in structure that are initiated from rehybridization of the imidazolidine N10 atom and are mostly limited to the conversion of the imidazolidine ring from a nearly planar to half-chair conformation, and to the twist that pushes the aromatic PABA ring out of plane occupied by the imidazolidine ring (Figures 3 and 4). Thus, the entropy contribution for both conformers of the mTHF molecule is very similar and will not be considered in calculating relative free energies.

Comparison of the results in Table 2 indicates that in aqueous solution the flat and bent *solution* mTHF forms have very similar total free energies represented either by the $G(PB)_{subtotal}$ or by $G(GB)_{subtotal}$ terms. These results interestingly correspond to the experimental study of the mTHF molecule carried out using the ^1H NMR spectrum analysis and model building in solution [34]. In that study, the authors observed no evidence of the effect of the pyrimidine ring-current field on the hydrogens of the PABA ring. That observation, together with some model-determined consideration, brought them to the conclusion that the PABA ring is bonded to imidazolidine N10 so as to go away from the pterin ring, rather than 'fold back' toward it. This means that the conformation of the mTHF molecule in solution is relatively flat, rather than bent. However, the authors of that study declared that this conclusion might not be true at neutral pH range, since the ring-current field effect might be cancelled out by diamagnetic anisotropy of the carbonyl C4 to O4 double bond. Thus, a dominant conformation in the neutral pH range has not been firmly determined. In this context, our results do not contradict the findings in the referred study. Instead, based on the calculated total free energies, we suggest that there is no significant difference in population between flat and bent *solution* forms of the mTHF molecule in aqueous solution at neutral pH. Although our results should not be considered as being very exact values of the free energies, nevertheless, they show convincingly that there is little difference in energy between the flat and bent *solution* mTHF conformers in aqueous solution;

therefore, both conformers should be in, or close to, equilibrium.

A closer inspection of the results in Table 2 reveals that, in spite of the very similar total free energies, the studied conformers differ in values of the individual free energy components. Thus, for the bent *solution* conformer the $E_{\text{electrostatic}}$ and E_{vdW} terms are more favorable than for the flat form by about 6 kcal/mol and 0.5 kcal/mol, respectively. On the other hand, the $G_{\text{solvation}}$ term stabilizes more the flat form compared to the bent *solution* form by about 3 kcal/mol. In addition, the flat conformer has a lower contribution from the E_{internal} term than the bent *solution* form by about 3.5 kcal/mol. In the result, a free energy contribution of 6.5 kcal/mol favoring the bent *solution* over flat form due to the $E_{\text{electrostatic}}$ and E_{vdW} terms is fully counterbalanced by the $G_{\text{solvation}}$ and E_{internal} contributions that together favor the flat over bent *solution* form by a similar amount of 6.5 kcal/mol, resulting in almost zero final free energy difference between both forms. In the following paragraphs we will briefly analyze those differences in the free energy terms.

The difference in E_{internal} term favoring the flat over bent *solution* form may probably be explained by less favorable torsion interactions around the N10-C4' bond in the bent *solution* form, resulted from a somewhat strained PABA-imidazolidine ring system in this form (Figures 3 and 4). That strain effect is a consequence of rehybridization of the imidazolidine N10 atom from sp^2 in the flat to sp^3 in bent *solution* conformation. The difference in E_{vdW} term is quite small and cannot be easily rationalized, since there are no individual steric contacts that would substantially disfavor one form in relation to the other. The less neutral partial charges on the atoms around N10 in the bent *solution* form compared to the flat one (Table 1) produce more favorable electrostatic energies, reflected by more favorable $E_{\text{electrostatic}}$ term in the bent *solution* form compared to flat one. Since the effect of electrostatic solvation is to a large extent to screen internal electrostatic interactions, thus corresponding $G_{\text{solvation}}$ contributions favoring the flat form counterbalance in part the $E_{\text{electrostatic}}$ energies that favor the bent *solution* form. Among factors describing the solvating effect, the values of SASA term are similar for both forms and amount to 751.1 Å^2 and 748.8 Å^2 for the bent *solution* and flat forms of the mTHF molecule, respectively. The dipole moments calculated from the distribution of the RESP atomic charges are equal to 71.7 D for flat mTHF and 63.4 D for bent *solution* mTHF. Therefore, the mTHF molecule interacts more favorably with the water molecules in its flat compared to bent *solution* form, as reflected by the $G(\text{PB})_{\text{solvation}}$ and $G(\text{GB})_{\text{solvation}}$ terms, both favoring the flat form by about 3 kcal/mol. In addition, our results confirm a very well known in literature fact of very good agreement of calculated solvation free energies obtained from two independent solvation models: the generalized Born method and more computationally demanding the Poisson–Boltzmann approach [28, 57–60].

Another approach to analyze results of our calculations is to examine the RESP atomic charges. The RESP charges have been shown to accurately represent the electrostatic interactions as well as the dipole moment of the molecule. The constraints in the RESP method were especially designed for avoiding instability during the fitting procedure. It was shown that RESP method produces charges that are much less conformation dependent than other methods [61, 62]. Thus, if the differences found in charges for flat and bent *solution* forms of the mTHF molecule are large this means that such difference should be considered significant.

The RESP charges in the flat form are quite similar to the corresponding charges in the bent *solution* form in most parts of the mTHF molecule (Table 1). One exception is a large difference between the charges on the N10 atom. In the flat form, we may expect a resonance through the PABA ring. That resonance would extend from the sp^2-hybridized N10 atom on one side to the electron-accepting CONHR group on the other side of the PABA ring. Thus, the N10 atom in the flat conformation has a very small negative charge of about −0.08, as the most of the electron density of its free π-electron pair would be engaged in the resonance. Due to a change of hybridization to sp^3 type, the N10 atom in the bent *solution* conformation has its orbitals in different orientation and is not able to contribute to the resonance effect; hence its atomic charge is more negative and equal to −0.53. In this case, the charges on atoms located near the N10 atom are also affected. Actually, we observe increased differences in charge between the

flat and bent *solution* forms of the mTHF molecule on those atoms that contribute to the resonance (C4′, C1′, and C), as well as those, which are located on the opposite side of the N10 atom such as C11, N5, and C9 in the imidazolidine ring, as well as C8A and N8 in the pterin part of the molecule. It is important to note that the resonance effect occurring in the flat conformation should lower the aromaticity of the PABA ring due to an increase of the π-electron localization in the conjugated system (Figure 6). On the contrary, the PABA ring in the bent *solution* conformation should have more aromatic and presumably more hydrophobic character. Then, according to one of the most common concepts defining the aromaticity effect [63], a higher aromatic character would mean an enhanced stability of the PABA ring in the bent *solution* form of the mTHF molecule. On the other hand, an increase in hydrophobic character of the PABA ring should slightly disfavor the bent *solution* form due to a weaker solvation of this fragment of the molecule (see $G(\mathrm{PB})_{\mathrm{solvation}}$ and $G(\mathrm{GB})_{\mathrm{solvation}}$ in Table 2).

Besides the basic calculations, where the ionic strength in solution was kept zero, the supplementary linear PB calculations were performed in order to estimate the free energy changes upon addition of salt. We examined dependency of the solvation free energy on two monovalent salt concentrations: 0.1 M and 1.0 M. The results (not shown) clearly indicate that the solvation free energies for the *solution* forms of the mTHF molecule are almost independent on the salt concentration in a broad range up to 1 M.

Implications on cofactor binding in thymidylate synthase reaction

While the results of our simulations show that in aqueous solution the flat and bent *solution* mTHF forms have very similar free energies, it would be of interest to find out, if and how this equilibrium changes upon binding to thymidylate synthase active site. It is clear that upon binding to the enzyme, the mTHF molecule undergoes desolvation and a respective change in $G_{\mathrm{solvation}}$ should be observed. That process intensifies when the active site is upon closing and the ligands are sequestered from bulk solvent. On the other hand, when the cofactor binds initially to TS, the spacious active site of the enzyme is open and still filled with many water molecules. Given that rationale, we may expect a strong dependence of conformation of the mTHF molecule on the desolvating effect in the closed active site. On the contrary, this dependence is relatively weak upon initial loose binding of the cofactor in a non-productive site in the open enzyme. In the following paragraphs we will analyze both situations and present our model for the conformational changes of the mTHF molecule during its progressive binding to TS.

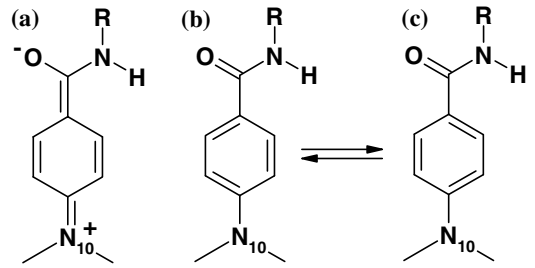

Figure 6. Canonical structures illustrating the resonance through the PABA ring in the mTHF molecule. *b* and *c* represent the hypothetical Kekule structures, which, if in equilibrium, add up to a fully aromatic hybrid, where the π-electrons are delocalized among all atoms in the ring. *a* is a hypothetical canonical structure showing the π-electron arrangement in the presence of the cross-conjugation effect. *a* would expectedly have a substantial contribution to the hybrid of *a*, *b*, and *c* for the flat form, but its occurrence is not possible for the bent form of the mTHF molecule. Contribution from the *a* structure lowers the aromaticity of the PABA ring, resulting from an increase in the π-electron (or double bond) localization in the ring.

First, we consider the loose adsorption binding of the cofactor in an initial non-productive site in the thymidylate synthase open conformer. Up to the present, there is very little evidence in the literature on cofactor conformation at this stage of the enzymatic reaction. Nonetheless, it is non-arguably assumed that the cofactor binds to the TS–dUMP non-covalent complex in its solution conformation with the imidazolidine ring closed [6, 7]. According to the results of our MM-PBSA calculations, the mTHF molecule may exist in aqueous solution at neutral pH as an equilibrium mixture of two forms: the flat, extended conformation where the PABA and imidazolidine rings are almost coplanar, and the slightly bent, more compact conformation, in which the PABA ring is twisted and approximately perpendicular to the imidazolidine ring (Figures 3 and 4). If our predic-

tion is correct, one may expect an occurrence of either form or both forms simultaneously at that early step of cofactor binding. The only evidence thus far known on cofactor closed-ring conformation in the open active site originates from the crystallographic structure of the ternary adsorption complex of the D169N mutant of *E.coli* TS with FdUMP and mTHF [64]. In that structure mutation in the enzyme prevented the closure of active site, which in turn resulted in two molecules of the cofactor bound in two partially occupied, non-productive binding sites. It is interesting that the conformations of those two molecules are noticeably different (Figure 7). In both molecules, the N10 atom is in sp^3-type hybridization and the imidazolidine ring adopts the half-chair conformation. However, one of those molecules, namely B, has nearly perpendicular orientation of the PABA with respect to imidazolidine ring, whereas in the other one, the A molecule, PABA is not rotated and is equatorial with respect to the imidazolidine ring. As a result, the A molecule is by 2 Å longer compared to the B one. Together, those molecules might be considered as two subsequent steps (A first, B next) on a 'conversion path' from the flat to bent *solution* form of the mTHF molecule. However, the conformations of the A and B molecules seem to correspond to the flat and bent *solution* conformations, respectively, to such extent, that A and B can even be considered as representatives of the conformational classes that are the same or closely related to those to which *solution* forms belong. Considering this, and in view of the results of our free energy calculations, we conclude that there is a strong possibility that neither flat nor bent *solution* form of the mTHF molecule would be clearly favored at the time of initial binding of the ligands to the open enzyme conformer. The open enzyme conformer can accommodate the both forms and selection of one of them for further steps in reaction does probably not occur before the active site starts closing.

The initial association of the cofactor produces a loosely bound ternary complex, which is next converted to the productive tightly bound intermediate. We propose that this conversion does not involve an opening of the cofactor imidazolidine ring and is accompanied by a cofactor transition from its initially bound form to the bent *enzyme* form. This last form, which is shown in Figure 2, has been predicted in Hyatt et al. [5] and recently found in preliminary crystallographic study of the structure of the covalent ternary complex between TS, the substrate analogue 5-nitro-dUMP, and mTHF [40]. According to our model, at the time of initial binding the cofactor molecule remains in equilibrium (or close to equilibrium) of extended and slightly bent conformations, models of which are the flat and bent *solution* forms, respectively (Figures 3 and 4). Then, upon the conformational change of the enzyme leading to the closure of the active site, the ligands are under a strong desolvating effect so the mentioned equilibrium should change. Analysis of the results in Table 2 demonstrates that if the solvating effect is not taken into account i.e., in the case of the fully desolvated molecules, the total free energy (represented by E_{gas}) is lower for the bent *solution* form of the mTHF molecule and this form should be more abundant in such environment (gas phase). Obviously, an estimation of the desolvating effect in protein active site by means of a comparison between free energies in aqueous solution and in gas phase would be hardly recognized as a satisfactory model. Nevertheless, when trying to anticipate consequences of the desolvating effect on the mTHF molecule, we may assume that the flat form, which has more favorable solvation free

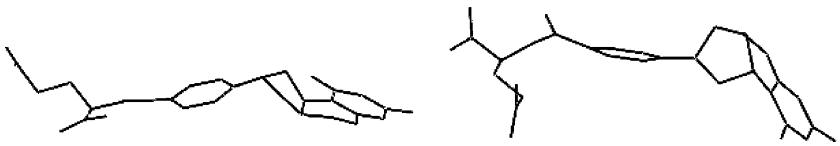

Figure 7. *a* (left) and *b* (right) molecules of mTHF found in an open active site of the ternary complex of the D169N mutant of *E.coli* TS with dUMP and mTHF.[61] Hydrogen atoms are omitted. The *a* molecule is in extended conformation and is 2 Å longer than the *b* molecule, which is approximately C-shaped bent. Therefore, the *a* molecule resembles the flat form, whereas the *b* molecule is similar to the bent *solution* form of the mTHF molecule. However, the *a* and *b* molecules may as well be considered as two 'sequences' of the conversion from the flat to bent *solution* form, with *a* (where imidazolidine N10 atom is sp^3-hybridized but PABA is not twisted) preceding *b* (where PABA is perpendicularly twisted with respect to imidazolidine).

energy (Table 2), would have to pay a higher desolvation price upon binding to TS compared to the bent *solution* form. To illustrate that prediction we carried out additional continuum solvent calculations using the Poisson–Boltzmann model. The interior dielectric constant of the mTHF *solution* forms was assigned value of 4, which is a protein interior like value, and the surrounding medium was assigned to a dielectric constant equal to water like value of 80. Assuming that the other contributions to the free energy are constant, the corresponding total $G(PB)_{subtotal}$ free energies were then equal to −90.71 and −92.96 kcal/mol for the flat and bent *solution* forms, respectively, favoring the bent *solution* form by above 2 kcal/mol. Although that may only be considered a very simple approximation of the desolvating effect where desolvation depends purely on the change in dielectric, it supports our assumption that the bent *solution* form of the mTHF molecule would emerge as being more stabilized compared to flat form at the time of the conformational change of the enzyme i.e., when the ligands are desolvated. Furthermore, the bent *solution* form fits much looser but without steric clashes if substituted for the bent *enzyme* conformer in the closed active site of the TS–NO_2dUMP–mTHF ternary complex [40], whereas the flat form of the mTHF molecule is too long and does not fit to any of the known geometries of the closed TS active site [5, 37]. Based on those arguments, we predict that the conformational equilibrium for the mTHF forms would be shifted toward the bent *solution* form during the binding process when desolvation takes place. It should be added that the charge–charge interactions with the protein may also play some role in this shift in equilibrium but they are probably less important at this step since the charges of both competing forms are mostly similar and the loose complex produces less directional and thus relatively weak electrostatic interactions. (Such interactions, however, have a strong directional character and play an important role in the closed enzyme.) Since in our model the bent *enzyme* conformation is proposed as an ultimate form of the unaltered cofactor in the ternary complex, in the next paragraph we will examine differences between the structures of the bent *solution* and bent *enzyme* forms. We will try to find out the rationale behind those differences in view of conformational adjustments required for productive binding and covalent reaction of the cofactor in the closed TS active site in the ternary complex.

The structure of the bent *enzyme* form demonstrates several modifications compared to the structure of the bent *solution* conformer, with the former form being more strained (Figure 8). This 'additional strain', or additional bending, appears to work as a perfect structural adaptation that aids the tight binding of the *enzyme* form of mTHF in a seemingly preformed hole in the closed TS active site [40]. Also, the strain exposes more the lone pair of electrons on the N10 atom, which may result in an increased basicity of this atom. This would promote the protonation of the N10 atom, which in turn would lead to the opening of the imidazolidine ring and subsequent formation of the covalent ternary complex (see Figure 1, step 2). Our preliminary results of the pK_a calculations support such possibility by providing arguments for an elevated pK_a of the N10 atom in the active site of the TS ternary complex with 5-nitro-dUMP and mTHF [65]. In addition, we propose that the change from the bent *solution* to bent *enzyme* form does not require large free energy compensation. Our molecular dynamics simulations of the bent *enzyme* system, carried out with maintaining the

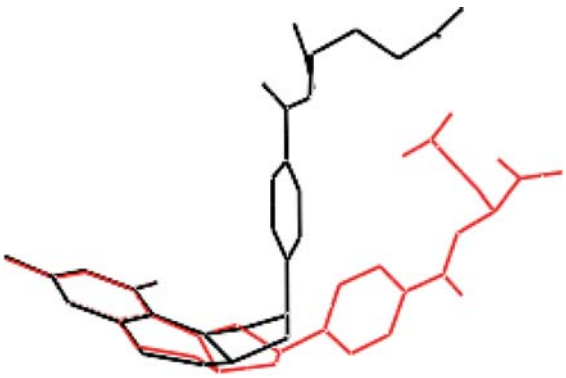

Figure 8. Superposition of the bent *solution* (red) with bent *enzyme* (black) conformation of the mTHF molecule. Hydrogen atoms are omitted for clarity. The *enzyme* molecule is in the strongly bent, L-shaped conformation. Such conformation imposes a strain on the imidazolidine ring. Most of that strain is relieved in the *solution* form. In both forms, the presence of the sp^3 orbital on the N10 atom resulted in the PABA ring being twisted and well out of the plane of the imidazolidine ring. This is in contrast to the coplanar arrangement of both rings in the flat form. Therefore, upon transition from the bent *solution* to bent *enzyme* form, no energy contributions are required neither for rehybridization of N10 nor for breaking the conjugation in the π-orbital system between N10 and the PABA ring (see text).

same conditions as those used in the calculations involving the flat and bent *solution* forms of the mTHF molecule, seem to support such conclusion. They show that in aqueous solution the bent *enzyme* form is undergoing a spontaneous partial 'unfolding' and is converted to a form similar to the bent *solution* conformer (except that the glutamate moiety has the carboxylic chains reversed in position compared to *solution* form) during less than 200 ps of simulation time. The occurrence of such conversion and its fairly short duration prove that the bent *enzyme* and bent *solution* forms belong to similar conformational classes, with the change from one class to the other depending on the character of host medium (closed TS enzyme against aqueous solution). This means that the conformational class represented by the bent *solution* form can be considered to be equivalent to class represented by the bent *enzyme* conformer, the first class being favored by interactions with water molecules in the uniform water medium, and the second resulting from the structural modifications caused by specific local interactions in the productive site in protein interior. Therefore, we think that the transition from the bent *solution* form to the catalytically active bent *enzyme* form, which would take place upon cofactor burying in the productive site, can be considered a 'required' and energetically not expensive process. That process is likely to be driven by numerous specific contacts with protein available in the productive site [40], which yield the strained and prone to reaction cofactor tightly bound in the ternary complex with TS and substrate.

Conclusions

In the current paper we use molecular dynamics, along with post-processing with the MM-PBSA method, to compare in detail (in part quantitatively) the three conformational forms the cofactor adopts during the thymidylate synthase catalyzed reaction: flat, bent *solution*, and bent *enzyme*. We show that in solution, in the neutral pH range, the *flat* and bent *solution* forms remain in equilibrium. The bent *solution* conformer has a lower intramolecular electrostatic energy, whereas flat form is the one that is more favorably solvated.

We integrate the results of our study with crystallographic and kinetic data suggesting the unaltered mTHF molecule (imidazolidine ring closed) is bound in the ternary complexes, to propose a novel model for progressive binding of the cofactor to TS during catalysis. In this model, we designate an important role in the binding mechanism for the bent *solution* form. Our model addresses controversies in the literature (discussed in the Introduction) concerning the mechanism by which the cofactor molecule is transformed from its solution conformation into the (strongly bent) derivative form with broken imidazolidine ring seen in covalent ternary complexes of TS. At the core of our model is the following: (i) the existence of the bent *solution* form at early steps of binding of the cofactor to TS, and (ii) the conversion from the bent *solution* to bent *enzyme* form during further steps, i.e. upon the desolvation of the ligands and burying of the cofactor in the closed TS active site. In our model, binding progresses in the following way. The flat and bent *solution* forms are isoenergetic in solution and the open enzyme conformer can accommodate both. Upon the conformational change of the enzyme, the flat conformer is disfavored through the process of desolvation of ligands and the bent *solution* form prevails. The latter form undergoes further bending into the bent *enzyme* conformation (with intact imidazolidine ring) upon full closure of the active site. Our calculations indicate that this conformation is energetically accessible, despite being strained, leading to an arrangement prone to reaction. The strain facilitates protonation at N10 [65], which, upon occurrence, promotes the opening of imidazolidine ring with subsequent formation of the reactive cation and, in turn, of the ternary covalent complex.

In this paper we present the conformational energetics of our model. Studies extending the foundation for this model, evaluating the protonation states of residues in the ternary complex, will follow [65].

Acknowledgements

This work was supported in part by Arizona Disease Control Research Commission Grant 20005 (to W.R.M.).

References

1. Pogolotti, A.L. Jr. and Santi, D.V., Bioorg. Chem., 1 (1977) 277.
2. Santi, D.V. and Danenberg, P.V., in Folates and Pterines, In Blakely, R.L. and Benkovic, S.J. (Eds.), Chemistry and Biochemistry of Folates 1. Wiley, New York, 1984, pp. 345–398.
3. Carreras, C.W. and Santi, D.V., Annu. Rev. Biochem., 64 (1995) 721.
4. Hardy, L.W., Acta Biochim. Pol., 42 (1995) 367.
5. Hyatt, D.C., Maley, F. and Montfort, W.R., Biochemistry, 36 (1997) 4585.
6. Montfort, W.R. and Weichsel, A., Pharmacol. Ther., 76 (1997) 29.
7. Stroud, R.M. and Finer-Moore, J.S., Biochemistry, 42 (2003) 239.
8. Finer-Moore, J.S., Santi, D.V. and Stroud, R.M., Biochemistry, 42 (2003) 248.
9. Myllykallio, H., Lipowski, G., Leduc, D., Filee, J., Forterre, P. and Liebl, U., Science, 297 (2002) 105.
10. Cohen, S.S., Ann. NY Acad. Sci., 186 (1971) 292.
11. Ealick, S.E. and Armstrong, S.R., Curr. Opin. Struct. Biol., 3 (1993) 861.
12. Lewis, C.A. Jr. and Dunlap, R.B., In Burgen, A.S.V. and Roberts, G.C.K. (Eds.), Topics in Molecular Pharmacology.. Elsevier/North-Holland Biomedical, New York, 1981, pp. 170–219.
13. Jackman, A.L., Jones, T.R. and Calvert, A.H., In Muggia, F.M. (Ed), Experimental and Clinical Progress in Cancer Chemotherapy. Martinus Nijhoff Publishers, Boston, 1985, pp. 155–210.
14. Eckstein, J.W., Foster, P.G., Finer-Moore, J., Wataya, Y. and Santi, D.V., Biochemistry, 33 (1994) 15086.
15. Rode, W., Zieliński, Z., Dzik, J.M., Kulikowski, T., Bretner, M., Kierdaszuk, B., Cieśla, J. and Shugar, D., Biochemistry, 29 (1990) 10835.
16. Dzik, J.M., Bretner, M., Kulikowski, T., Gołos, B., Jarmuła, A., Poznański, J., Rode, W. and Shugar, D., Biochim. Biophys. Acta, 1293 (1996) 1.
17. Smith, G.K., Amyx, H., Boytos, C.M., Duch, D.S., Ferone, R. and Wilson, H.R., Cancer Res., 55 (1995) 6117.
18. Beale, P. and Clark, S., In Jackman, A.L. (Ed), Anticancer Drug Development. Humana Press, Inc., Totowa, NJ, 1999, pp. 167–181.
19. Webber, S., Bartlett, C.A., Boritzki, T.J., Hillard, J.A., Howland, E.F., Johnston, A.L., Kosa, M., Margosiak, S.A., Morse, C.A. and Shetty, B.V., Cancer Chemother. Pharmacol., 37 (1996) 509.
20. Shih, C. and Thornton, D.E., In Jackman, A.L. (Ed), Anticancer Drug Development. Humana Press, Inc., Totowa, NJ, 1999, pp. 183–201.
21. Shoichet, B.K., Perry, K.M., Santi, D.V., Stroud, R.M. and Kuntz, I.D., Science, 259 (1993) 1445.
22. Costi, M.P., Rinaldi, M., Tondi, D., Pecorari, P., Barlocco, D., Ghelli, S., Stroud, R.M., Santi, D.V., Stout, T.J., Musiu, C., Marangiu, E.M., Pani, A., Congiu, D., Loi, G.A. and La Colla, P., J. Med. Chem., 42 (1999) 2112.
23. Stout, T.J., Tondi, D., Rinaldi, M., Barlocco, D., Pecorari, P., Santi, D.V., Kuntz, I.D., Stroud, R.M., Shoichet, B.K. and Costi, M.P., Biochemistry, 38 (1999) 1607.
24. Tondi, D., Slomczynska, U., Ghelli, S., Watterson, D.M., Costi, M.P. and Shoichet, B.K., Chem. Biol., 6 (1999) 319.
25. Costi, M.P., Tondi, D., Rinaldi, M., Barlocco, D., Pecorari, P., Soragni, F., Venturelli, A. and Stroud, R.M., Biochim. Biophys. Acta-Mol. Basis Dis., 1587 (2002) 206.
26. Hartman, K.-R. and Heidelberger, C., J. Biol. Chem., 236 (1958) 3006.
27. Heidelberger, C., Prog. Nucl. Acid Res. Mol. Biol., 4 (1965) 1.
28. Srinivasan, J., Cheatham, T.E. III, Cieplak, P., Kollman, P.A. and Case, D.A., J. Am. Chem. Soc., 120 (1998) 9401.
29. Vorobjev, Y.N., Almagro, J.C. and Hermans, J., Proteins: Struct. Funct. Genet., 32 (1998) 399.
30. Jayaram, B., Sprous, D., Young, M.A. and Beveridge, D.L., J. Am. Chem. Soc., 120 (1998) 10629.
31. Kollman, P.A., Massova, I., Reyes, C., Kuhn, B., Huo, S., Chong, L., Lee, M., Lee, T., Duan, Y., Wang, W., Donini;, O., Cieplak, P., Srinivasan, J., Case, D.A. and Cheatham, T.E. III, Acc. Chem. Res., 33 (2000) 889.
32. Finer-Moore, J., Montfort, W.R. and Stroud, R.M., Biochemistry, 29 (1990) 6977.
33. Matthews, D.A., Appelt, K., Oatley, S.J. and Xuong, N.H., J. Mol. Biol., 214 (1990) 923.
34. Poe, M., Jackman, L.M. and Benkovic, S.J., Biochemistry, 18 (1979) 5527.
35. Tamelen, E.E. and Hopla, R.E., J. Am. Chem. Soc., 101 (1979) 6114.
36. Santi, D.V., McHenry, C.S., Raines, R.T. and Ivanetich, K.M., Biochemistry, 26 (1987) 8606.
37. Matthews, D.A., Villafranca, J.E., Janson, C.A., Smith, W.W., Welsh, K. and Freer, S., J. Mol. Biol., 214 (1990) 937.
38. Spencer, H.T., Villafranca, J.E. and Appleman, J.R., Biochemistry, 36 (1997) 4212.
39. Eldin, S. and Jencks, W.P., J. Am. Chem. Soc., 117 (1995) 4851.
40. Arendall, B. and Montfort, W.R., in press .
41. Insight II version 2.2.0, Biosym Technologies (1993), San Diego, CA.
42. Case, D.A., Pearlman, D.A., Caldwell, J.W., Cheatham, T.E. III, Ross, W.S., Simmerling, C.L., Darden, T.A., Merz, K.M., Stanton, R.V., Cheng, A.L., Vincent, J.J., Crowley, M., Tsui, V., Radmer, R.J., Duan, Y., Pitera, J., Massova, I., Seibel, G.L., Singh, U.C., Weiner, P.K. and Kollman, P.A. AMBER 6. University of California, San Francisco, 1999.
43. Cornell, W.D., Cieplak, P., Bayly, C.I., Gould, I.R., Merz, K.M., Ferguson, D.M., Spellmeyer, D.C., Fox, T., Caldwell, J.W. and Kollman, P.A., J. Am. Chem. Soc., 117 (1995) 5179.
44. Jorgensen, W.L., J. Chem. Phys., 77 (1992) 5757.
45. Essmann, U., Perera, L., Berkowitz, M.L., Darden, T., Lee, H. and Pedersen, L.G., J. Chem. Phys., 103 (1995) 8577.
46. York, D.M., Darden, T.A. and Pedersen, L.G., J. Chem. Phys., 99 (1993) 8345.
47. Gaussian 98 (Revision A.1), Frisch, M.J., Trucks, G.W., Schlegel, H.B., Scuseria, G.E., Robb, M.A., Cheeseman, J.R., Zakrzewski, V.G., Montgomery, Jr., J.A., Stratmann, R.E., Burant, J.C., Dapprich, S., Millam, J.M., Daniels, A.D., Kudin, K.N., Strain, M.C., Farkas, O., Tomasi, J., Barone, V., Cossi, M., Cammi, R., Mennucci, B., Pomelli, C., Adamo, C., Clifford, S., Ochterski, J.,

Petersson, G.A., Ayala, P.Y., Cui, Q., Morokuma, K., Malick, D.K., Rabuck, A.D., Raghavachari, K., Foresman, J.B., Cioslowski, J., Ortiz, J.V., Baboul, A.G., Stefanov, B.B., Liu, G., Liashenko, A., Piskorz, P., Komaromi, I., Gomperts, R., Martin, R.L., Fox, D.J., Keith, T., Al-Laham, M.A., Peng, C.Y., Nanayakkara, A., Gonzalez, C., Challacombe, M., Gill, P.M.W., Johnson, B.G., Chen, W., Wong, M.W., Andres, J.L., Head-Gordon, M., Replogle, E.S. and Pople, J.A., Gaussian, Inc., Pittsburgh PA, 1998.

48. Bayly, C.I., Cieplak, P., Cornell, W.D. and Kollman, P.A., J. Phys. Chem., 97 (1993) 10269.
49. Cieplak, P., Bayly, C.I., Cornell, W.D. and Kollman, P.A., J. Comput. Chem., 16 (1995) 1357.
50. Honig, B., Sharp, K. and Yang, A.-S., J. Phys. Chem., 97 (1993) 1101.
51. Sharp, K.A. and Honig, B., Annu. Rev. Biophys. Biophys. Chem., 19 (1990) 301.
52. Honig, B. and Nicholls, A., Science, 268 (1995) 1144.
53. Still, W.C., Tempczyk, A., Hawley, R.C. and Hendrickson, T., J. Am. Chem. Soc., 112 (1990) 6127.
54. Jayaram, B., Sprous, D. and Beveridge, D.L., J. Phys. Chem. B, 102 (1998) 9571.
55. Sitkoff, D., Sharp, K.A. and Honig, B., J. Phys. Chem., 98 (1994) 1978.
56. Sanner, M.F., Spehner, J.-C. and Olson, A.J., Biopolymers, 38 (1996) 305.
57. Srinivasan, J., Trevathan, M.W., Beroza, P. and Case, D.A., Theor. Chem. Acc., 101 (1999) 426.
58. Qiu, D., Shenkin, P., Hollinger, F. and Still, W., J. Phys. Chem. A, 101 (1997) 3005.
59. Edinger, S.R., Cortis, C., Shenkin, P.S. and Friesner, R.A., J. Chem. Phys. B, 101 (1997) 1190.
60. Dominy, B.N. and Brooks, C.L. III, J. Phys. Chem. B, 103 (1999) 3765.
61. Cornell, W.D., Cieplak, P., Bayly, C.I. and Kollman, P.A., J. Am. Chem. Soc., 115 (1993) 9620.
62. Howard, A.E., Cieplak, P. and Kollman, P.A., J. Comput. Chem., 16 (1995) 243.
63. Minkin, V.I., Glukhovtsev, M.N. and Simkin, B.Ya. Aromaticity and Antiaromaticity: Electronic and Structural Aspects. Wiley, New York, 1994.
64. Sage, C.R., Michelitsch, M.D., Stout, T.J., Biermann, D., Nissen, R., Finer-Moore, J. and Stroud, R.M., Biochemistry, 37 (1998) 13893.
65. Jarmuła, A., Cieplak, P. and Montfort, W.R., in press .